JPE 4-1-6

ZVS-PWM Boost Chopper-Fed DC-DC Converter with Load-Side Auxiliary Edge Resonant Snubber and Its Performance Evaluations

Koki Ogura[†], Srawouth Chandhaket, Tarek Ahmed and Mutsuo Nakaoka

Department of Electrical and Electronics Engineering, The Graduate School of Science
and Engineering, Yamaguchi University

ABSTRACT

This paper presents a high-frequency ZVS-PWM boost chopper-fed DC-DC converter with a single active auxiliary edge resonant snubber in the load-side which can be designed for power conditioners such as solar photovoltaic generation, fuel cell generation, battery and super capacitor energy storages Its principle operation in steady-state is described in addition to a prototype setup. The experimental results of ZVS-PWM boost chopper–fed DC-DC converter proposed here, are evaluated and verified with a practical design model in terms of its switching voltage and current waveforms, the switching v-i trajectory, the temperature performance of IGBT module, the actual power conversion efficiency and the EMI of radiated and conducted emissions. And then discussed and compared with the hard switching scheme from an experimental point of view Finally, this paper proposes a practical method to suppress parasitic oscillation due to the active auxiliary resonant switch at ZCS turn off mode transition with the aid of an additional lossless clamping diode loop, and reduced the EMI conducted emission in this paper.

Keywords　DC-DC converter, Active auxiliary edge-resonant snubber, Zero voltage soft switching (ZVS), PWM, v-i switching trajectory representation, EMI noise evaluations, Parasitic oscillation under ZCS turn-off

1. Introduction

In recent years, the higher efficiency, the more advanced power conversion, energy utilization equipment and a variety of circuit topologies of the soft-switching DC-DC power converter are urgently required. The practical developments of isolated or non-isolated DC-DC power converter using power semiconductor devices have attracted special interest in various fields related to the alte

-rnative and renewable energy generation and power supplies of small-scale distributed type photovoltaic generation system, fuel cell generation system and battery and super capacitor energy storage systems for residential power energy applications, information and telecom munication equipment, and automobile power elect ronic applications including pure electric vehicle (EV) and hybrid EV systems Because of the high-frequency switching PWM technologies with the great advances of power semiconductor devices such as power MOSFETs, IGBTs, SITs, in addition to micropro cessor control board and the magnetic circuit comp onents of inductor and transformer, the DC-DC power converters have been

strongly demanded miniaturization in size, lighter in weight, and high performances (high-speed response, and waveform quality) However, the significant problems for the high-frequency switching PWM power conversion technologies cause system efficiency reduction due to increased switching losses and snubber circuit losses, the higher dv/dt and di/dt electrical surge stresses, high frequency leak current to the ground and EMI noises, radiated emission and conducted emission. For effective and practical solutions, it is presently necessary to use the principles of soft-switching power conversion PWM techniques, which are based on active auxiliary edge resonant snubber[1]-[6] or passive edge resonant snubber[7][8]

In this paper, the circuit topology of the ZVS-PWM boost chopper-fed DC-DC power converter with a simple active auxiliary edge-resonant snubber is proposed. The experimental results of ZVS-PWM boost chopper-fed DC-DC power converter designed for the maximum 3kW output power, and switching frequency 16kHz are presented and discussed, together with comparative operating characteristics of this ZVS-PWM chopper-fed DC-DC power converter and conventional hard switching PWM one. In addition to these, this paper points out the practical method to protect a large voltage spike due to unnecessary and undersigned parasitic oscillation of the auxiliary resonant active power switch at ZCS turn-off commutation. This parasitic oscillation of this active resonant snubber can be suppressed with the aid of the simple lossless clamping diode connected with the auxiliary resonant snubber which can utilize at the load-side energy processing Furthermore, the practical effectiveness of this ZVS-PWM chopper-fed DC-DC power converter is substantially proved on the measured conducted EMI noise from an experimental point of view.

2. ZVS-PWM Boost Chopper-fed DC-DC Converter

2.1 Circuit Description

Fig 1 shows the circuit configuration of the proposed edge-resonant ZVS-PWM boost chopper-fed DC-DC power converter using IGBTs. This converter is based on the conventional PWM boost chopper-fed DC-DC power

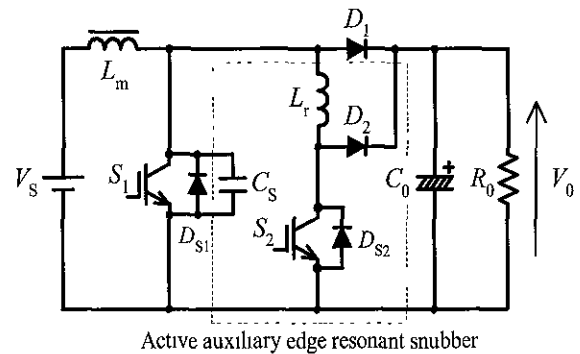converter, which also includes an active auxiliary resonant snubber circuit composed of a resonant

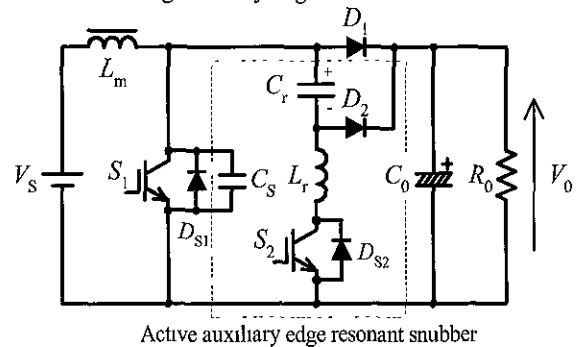Fig 1   ZVS-PWM Boost chopper-fed DC-DC converter using auxiliary edge resonant snubber

Fig 2. Boost ZVT-PWM converter [1]

inductor L_r, a resonant capacitor C_r, a lossless snubber capacitor C_s, an auxiliary active power switch S_2 and an auxiliary diode D_2. This DC-DC power converter is an improved circuit of [1] (see Fig 2). The converter circuit proposed in [1] has a problem which the auxiliary switch is turned off under hard switching However this auxiliary switch in the proposed ZVS-PWM boost chopper-fed DC-DC power converter can operate ZCS and ZVS in a turn-off transition by adding a resonant capacitor C_r.

2.2 Circuit Operation

The mode transition of ZVS-PWM boost chopper-fed DC-DC power converter are depicted in Fig. 3. The gate voltage pulse sequences of the main active power switch and the auxiliary active power switch are indicated in Fig. 4, the operating voltage and current waveforms of each component are shown in Fig 4. The operating principle in mode transitions of this chopper-fed DC-DC power converter is explained as follows,

Mode 0   The stored energy of the boost inductor L_m is transferred to the load side When the auxiliary power switch S_2 is turned on, Mode 0 changes to Mode 1
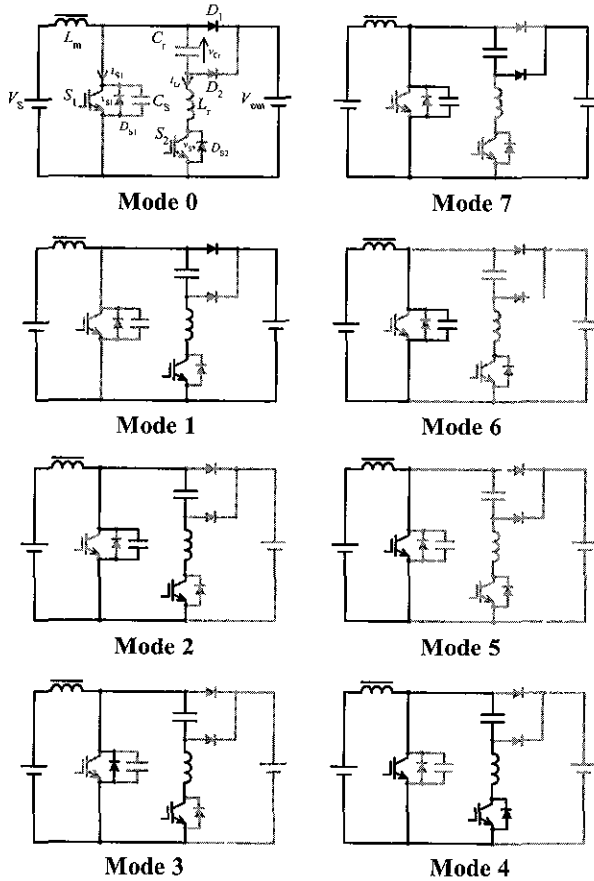

Fig 3   Mode transitions and equivalent circuits

Mode 1   When the auxiliary power switch S_2 is turned on with ZCS, the current through the diode D_1 begins to flow the active auxiliary resonant snubber circuit The current flow through the resonant inductor L_r, and the resonant capacitor C_r, and the auxiliary power switch S_2 increases sinusoidally

Mode 2   When the diode D_1 is turned off, the current flowing through D_1 commutates through the active auxiliary resonant snubber circuit The lossless snubber capacitor C_s connected in parallel with the main power switch S_1 is produced the edge-resonant mode with a resonant inductor L_r and resonant capacitor C_r Therefore, the lossless snubber capacitor C_s becomes the discharging mode, and the voltages across C_s drops gradually

(a) Gate voltage pulse sequences
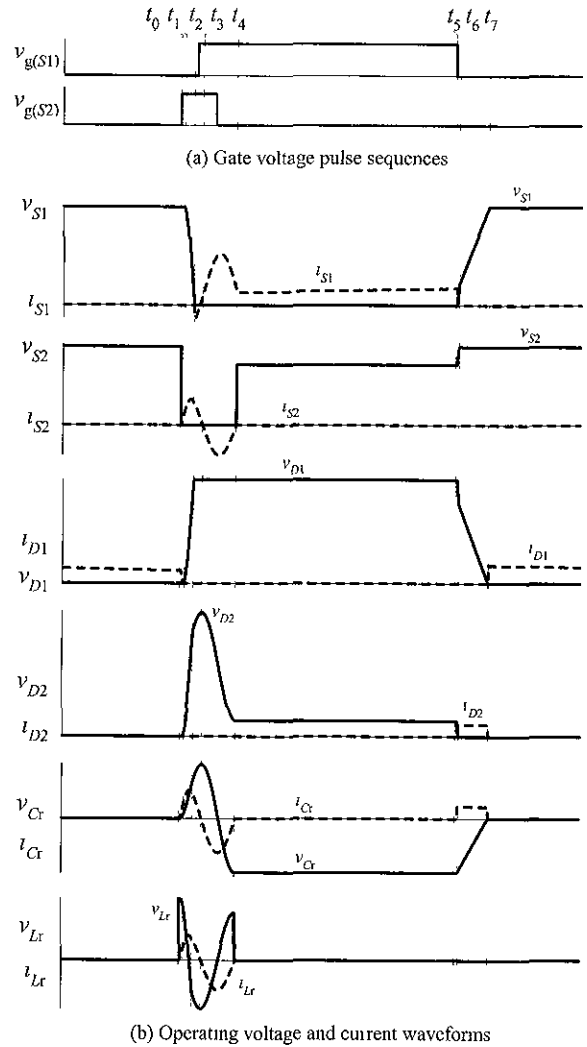
(b) Operating voltage and current waveforms

Fig 4   Gate pulse sequences and typical operating waveforms

Mode 3   When the voltage across the snubber capacitor C_s becomes zero, the anti-parallel diode D_{S1} of the main power switch S_1 is naturally turned on As a result, the main power switch S_1 can achieve ZVS and ZCS hybrid soft commutation in a turn-on transition when current flow through the anti-parallel diode D_{S1} decreases and naturally shifts to the main power switch S_1 by giving the gate voltage signal of the main power switch S_1 while D_{S1} is turned on

Mode 4   When the current of the main power switch S_1 becomes bigger than the current flowing through a boost inductor L_m, the diode D_{S2} in anti-parallel with the auxiliary power switch S_2 is naturally turned on, and the

current flowing through S_2 begins to commutate to the anti-parallel diode D_{S2}. By turning the gate voltage pulse signal delivered to the auxiliary power switch S_2 during this period, an auxiliary power switch S_2 can achieve complete ZVS and ZCS hybrid soft commutation in a turn-off transition when the current flowing through the auxiliary power switch S_2 shifts exactly.

Mode 5 When the auxiliary power switch S_2 is turned off, the resonant current flowing through the inductor L_r and the capacitor C_r becomes zero; all the circuit operations are identical to the conduction state of the conventional PWM boost chopper-fed DC-DC power converter.

Mode 6 When the main power switch S_1 is turned off with ZVS, the current flowing through the boost inductor L_m flows through the snubber capacitor C_s. Therefore, the lossless snubber capacitor C_s becomes its charging mode, and the voltages across the lossless capacitor C_s increases gradually.

Mode 7 When the voltage across the lossless snubber capacitor C_s becomes larger than the sum of the voltage across the resonant capacitor C_r and the output voltage V_o, the auxiliary diode D_2 is turned on. When the voltage across the lossless snubber capacitor C_s is equal to the output average voltage V_o and the voltage across the auxiliary resonant capacitor C_r becomes zero, the diode D_2 is naturally turned off. At the same time, the diode D_1 is turned on and Mode 7 shifts to Mode 0. This ZVS-PWM boost chopper-fed DC-DC power converter repeats cyclically the steady-state operation described above.

3. Experiment Results and Performance Evaluations

### 3.1 Design Specifications and Switching Operating Waveforms

The experimental design specifications and circuit parameter constants of the ZVS-PWM boost chopper-fed DC-DC power converter with a single active auxiliary edge-resonant snubber is listed in Table 1.

Fig. 5 (a) illustrates the voltage and current operating waveforms and its v-i trajectory in case of turn-on commutation of the main power switch S_1 of the hard

Table 1. Design specifications and circuit parameters.

DC Input Voltage	V_S	200V	Snubber Capacitor	C_S	33nF
DC Output Voltage	V_0	380V	Resonant Inductor	L_r	7.6μH
Switching Frequency	f_S	16kHz	Resonant Capacitor	C_r	121nF
Output Capacitor	C_0	8,200μF	Boost Inductor	L_b	1.02mH

(Remarks)
Power Switching Devices
. IGBT [S_1, S_2] – Mitsubishi CM75DU-24H
. Diode [D_1] – Toshiba 30JL2C41
. Diode [D_2] – Hitachi DFM30F12

switching PWM boost chopper-fed DC-DC power conv -erter in the hard switching. Fig. 5 (b) illustrates the voltage and current operating waveforms and its v-i trajectory in case of turn-on commutation of the main power switch S_1 of the ZVS-PWM one in the soft switching. From the voltage and current waveforms in
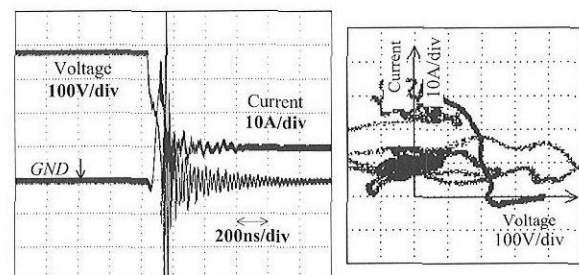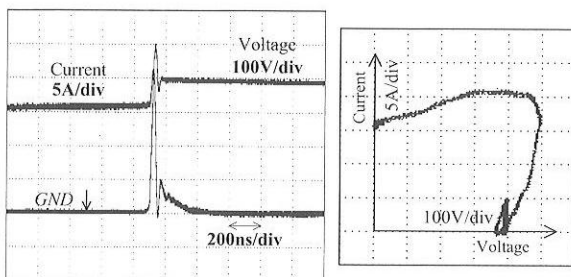

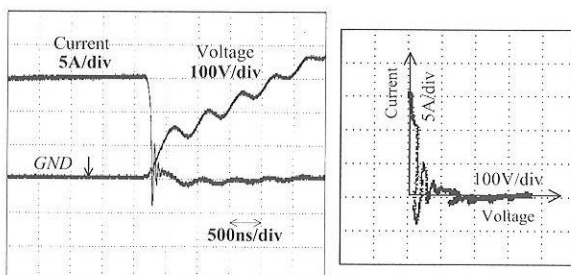(a) Hard switching scheme
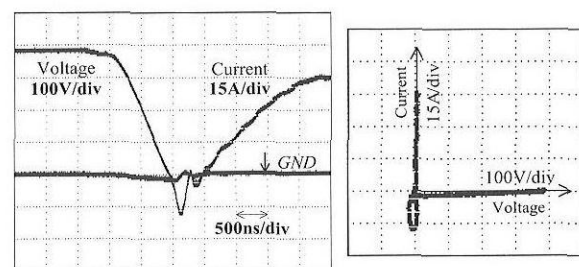
(b) Soft switching scheme

Fig. 5. Voltage and current waveforms and v-i trajectory in case of turn-on transition of main switch S_1.

Fig. 5 (a) under a condition of a hard switching comm. utation, the higher dv/dt and rapid di/dt characteristics as well as voltage surge and current surge can be observed. Moreover, taking a look at the v-i trajectory in Fig. 5 (a), it extends over the first quadrant and the second quadrant largely. Therefore, it is based on the increase of the electrical switching stresses for IGBT used in the converter, and increase of the switching

power loss and EMI noises. However, switching wave forms in Fig. 5 (b) under a condition of soft-switching commutation, the softened dv/dt and di/dt, and the suppression of the voltage surge and current surge can be achieved. Observing the v-i trajectory in Fig. 5 (b), it goes along the voltage axis and current axis of the main power switching device, so the ideal soft switching operation can be achieved without the switching losses at turn-on transition. Therefore, under the soft-switching scheme, the switching power losses, voltage surge and current surge don't occur because the switching can be achieved under a condition of ZVS and ZCS.

(a) Hard switching scheme

(b) Soft switching scheme

Fig. 6.   Voltage and current waveforms and v-i trajectory in case of turn-off transition of main switch S_1.

Fig. 6 (a) shows the voltage and current operating waveforms and its v-i trajectory in case of turn-off switching commutation in the hard switching. Fig. 6 (b) illustrates the voltage and current operating waveforms and its v-i trajectory in case of turn-off switching commutation in the soft-switching. From the voltage and current switching waveforms at turn-off comm. utation as depicted in Fig. 6 (a) under hard switching commutation, there is overlapped region of voltage and

current switching waveforms. Moreover, observing the v-i trajectory in Fig. 6 (a), it spreads out in the first quadrant in the v-i plane. Therefore, this concerns with increase of the switching power losses. Therefore, in Fig. 6 (b) under soft switching commutation, except for the overlapping period of the switching voltage and falling current during the turn-off period and tail current during the tail period of IGBT, there is no overlapping region. And taking a look at the v-i trajectory illustrated in Fig. 6 (b), it is nearly moving along the voltage axis and current axis of v-i plane. Therefore, under a soft-switching PWM scheme, the switching power losses of the power switch can be lowered as compared with that of the hard switching PWM scheme.

3.2 Temperature Characteristics of Main Power Switch

A small pin hole is under the metal bottom side of IGBT as the main switch S_1 power module package as shown in Fig. 7, and the tip of the K-type thermocouple probe is tightly inserted into the central portion of the IGBT module. The measured temperature of the 2 in 1 IGBT module package under a both operating conditions of the hard switching (H-SW) and soft-switching
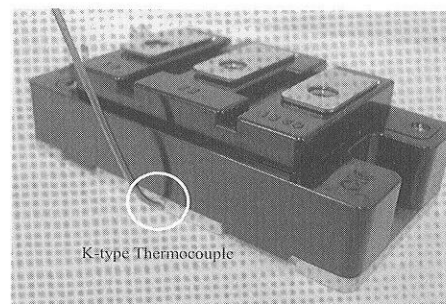

Fig. 7.   Temperature measurement of IGBT module using K-type thermocouple.

(S-SW) PWM schemes is depicted in Fig. 8.

As shown in Fig. 8, after 80 minutes of operation, the temperature of IGBT under hard switching scheme is 60°C, but the temperature under soft-switching scheme is 48°C. So soft-switching reduced temperature about 12°C as compared with hard switching scheme. In these results, the downsizing of the cooling equipment can be
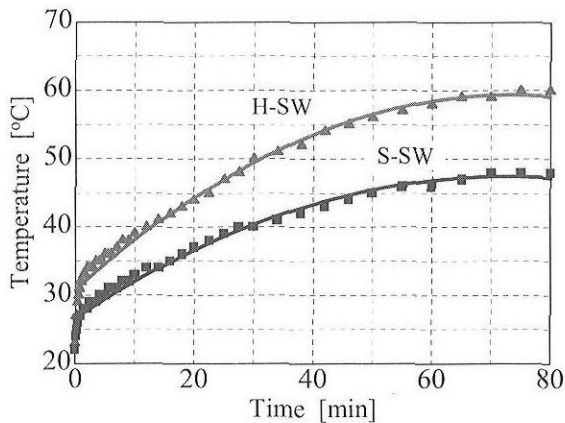
Fig. 8.　Temperature measurement of IGBT module.

substantially achieved, because the switching power losses of the main power switch S_1 can be sufficiently reduced with using ZVS-PWM scheme

3.3 Actual Power Conversion Efficiency Characteristics

The actual power conversion efficiency of hard switching PWM boost chopper-fed DC-DC power converter and soft switching ZVS-PWM one can be respectively measured by using the digital power meter.
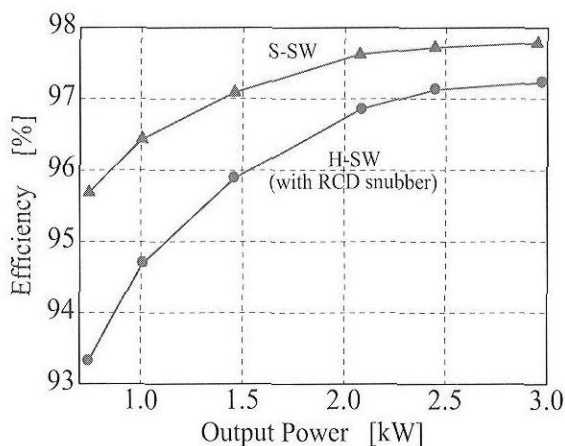

Fig. 9.　Output power vs. actual efficiency characteristics.

As the results in Fig. 9, the actual efficiency of the soft switching is higher than that of hard switching for the required output power range. Especially, for 3kW breadboard setup, the actual conversion efficiency of soft-switching PWM scheme achieves 97.8%. And moreover, for high frequency switching, this power circuit can achieve higher efficiency characteristics.

3.4 EMI Testing of Radiated Emissions

The performance of radiated emission measured by EMC bilog antenna (30MHz~1GHz) in the shielded anechoic chamber shown in Fig. 10.
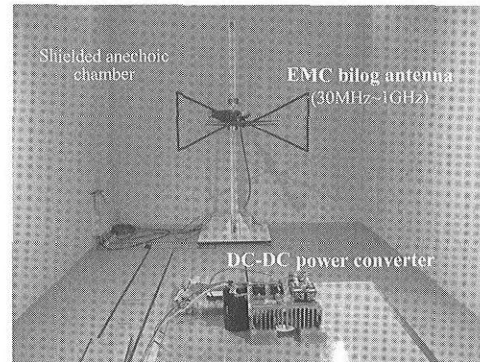

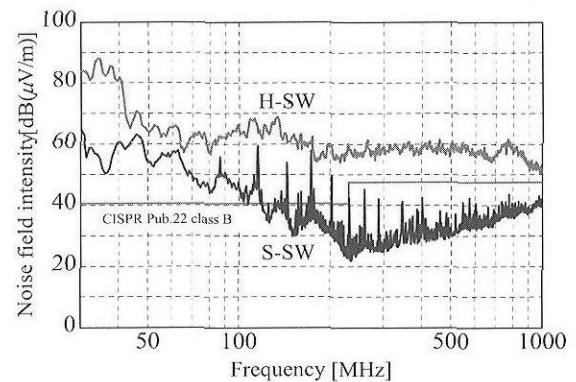Fig. 10.　Facility for measuring radiated emission.

Fig. 11.　Noise measurement of radiated EMI.

Observing from the results in Fig. 11, soft switching is lower noise level than that of hard switching for all over the frequency range. Especially, the noise level for the maximum 37.1 [dB □V/m] can be reduced at 230MHz. It is more effective to use the ZVS-PWM boost chopper-fed DC-DC power converter with active auxiliary resonant snubber to suppress the radiated emission.

3.5 EMI Testing of Conducted Emissions

The measuring result of conducted emission is measured with using the line impedance stabilization network (LISN) shown in Fig. 12[9][10]. According to the results in Fig. 13, soft switching is lower noise level than that of hard switching all over the frequency range
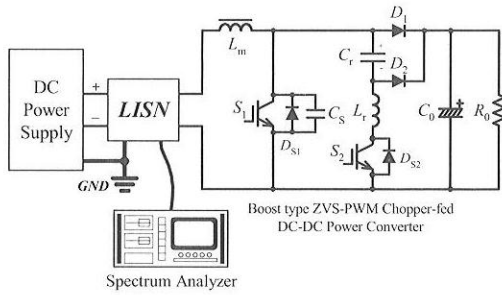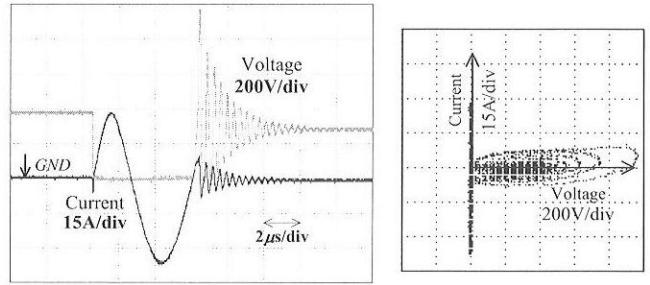
Fig. 12.   Measurement of conducted emission.

Fig. 13.   Noise measurement of conducted EMI.

Fig. 14.   Voltage and current waveforms and v-i trajectory of auxiliary switch S_2.

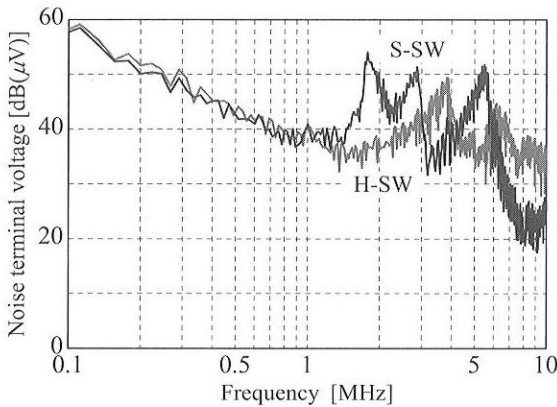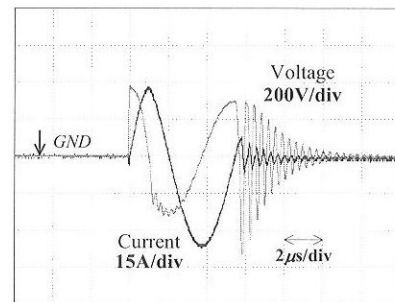Fig. 15.   Voltage and current waveforms of resonant inductor L_r

except for around 1.8MHz, 2.7MHz and 5.4MHz. Especially over 6MHz, soft switching can be excellent performance as compared with hard switching. It is effective to use a soft-switching PWM scheme with active auxiliary resonant snubber to suppress the conducted emission.

4. Parasitic oscillation of auxiliary power switch at ZCS turn-off

4.1 Generation of Parasitic Oscillation

Fig. 14 depicts a parasitic oscillation phenomenon at the voltage across the auxiliary power switch S_2 and its current waveforms at ZCS turn-off. This means that the quality factor of edge resonant circuit is high, and the element of dissipation is substantially small. This peak surge voltage across the auxiliary power switch S_2 becomes about 900V, so the power semiconductor device protection of the auxiliary power switch from a surge voltage is a significant problem.

Before the auxiliary power switch S_2 is turned off, the resonant current flowing through S_2 has naturally commut

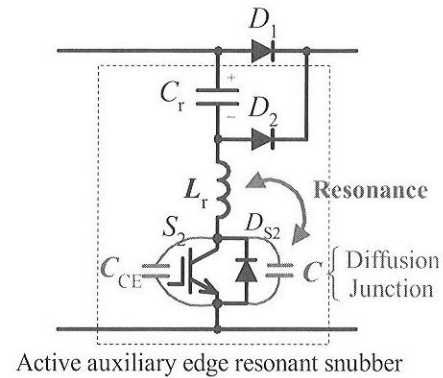Active auxiliary edge resonant snubber

Fig. 16.   Parasitic oscillation principle.

-ate to the antiparallel diode D_{S2}. During this interval, the gate voltage pulse signal of the auxiliary power switch S_2 has to be turned off. Presently, the resonant current flowing through the antiparallel diode D_{S2} becomes to zero if the diode D_{S2} is ideal. But in fact, the resonant current is not suppressed, and the reverse recovery current flowing through D_{S2} appears when changes from forward-directional bias to the reverse -directional bias.

The recombination and diffusion of the minority carrier is to be generated when the current direction

changed into the reverse direction from the forward direction. Due to the rapid direction change of current with a higher di/dt, a resonant inductor L_r connected to the auxiliary power switch S_2 in series induces a large voltage from the steep di/dt. So the voltage across the auxiliary power switch S_2 induces a large voltage, too. The voltage and current waveforms of the resonant inductor L_r at this time are shown in Fig. 15. The energy stored into that resonant inductor decreases with continuing resonant oscillation between the resonant inductor and the capacitor including collector-emitter capacitance C_{CE} of the auxiliary switch S_2, diffusion capacitance and junction capacitance of the antiparallel diode D_{S2} (See Fig. 16). Observing this oscillation frequency by using the synchroscope, it is about 2.7MHz. As compared with the results of synchroscope and the results of conducted emission shown in Fig. 13, it is proved that the fundamental frequency (about 2.7MHz) and the twice frequency (about 5.4MHz) appear as a spectrum due to this oscillation.

4.2 Suppression Method of Parasitic Oscillation

As for suppressing the parasitic oscillation, the clamping diode loop in the ZVS-PWM boost chopper-fed DC-DC power converter is added as illustrated in Fig. 17.
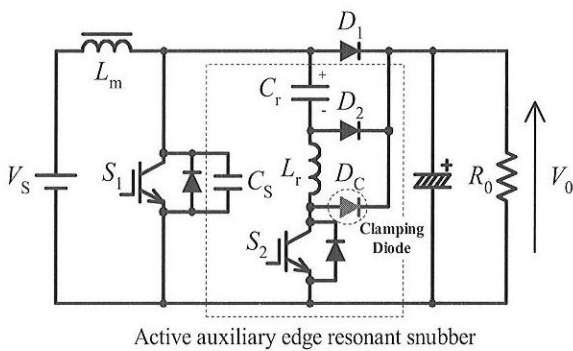

Fig. 17.   ZVS-PWM boost chopper-fed DC-DC converter with an additional clamping diode D_C.

This clamping diode with lossless snubber is naturally turned on when the voltage across the auxiliary power switch S_2 is higher than a voltage of the output DC port. Therefore, with using clamping diode loop can suppress the peak voltage across the auxiliary power switch S_2 less than the output voltage. And this snubber energy is used effectively at the output side, so lossless snubber can be implemented.
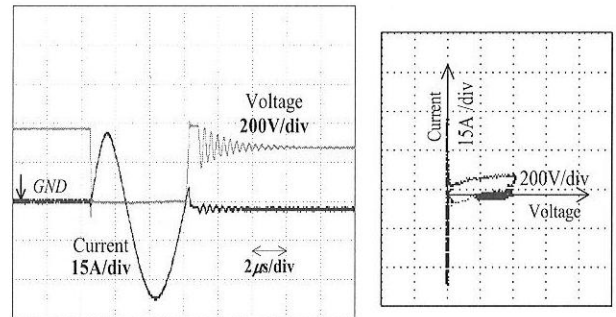

Fig. 18.   Voltage and current waveforms and v-i trajectory of auxiliary switch S_2 with a clamping diode.
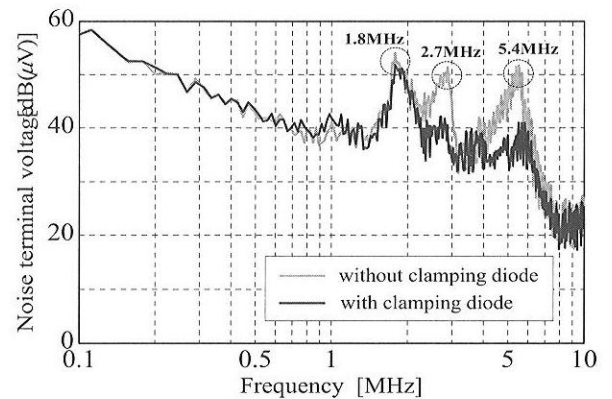

Fig. 19.   Comparative noise measurement of conducted EMI with a clamping diode and without clamping diode.

The voltage and current operating waveforms of the auxiliary power switch S_2 in case of adding a clamping diode are represented in Fig. 18. As shown in Fig. 18, a large oscillation in Fig. 14 disappears, and the surge voltage is effectively suppressed. Therefore, the over voltage across the auxiliary power switch S_2 can be reduced positively. Fig. 19 illustrates the measured result of conducted emission in case of using the clamping diode loop. According to Fig. 19, the noise level can reduce 5dB□V~10dB□V around 2.7MHz and 5.4MHz, therefore, excellent results are obtained for the suppression of the conducted emission.

5. Conclusions

In this paper, ZVS-PWM boost chopper-fed DC-DC power converter with a load side single active auxiliary resonant snubber has introduced for the power interface of the solar photovoltaic or fuel cell power conditioner.

The feasible characteristics of this ZVS-PWM boost chopper-fed DC-DC power converter using IGBTs is compared with the conventional hard switching PWM one on the basis of the voltage and current waveforms, switching v-i trajectory, measured temperature of IGBT module package, actual power conversion efficiency, and EMI test data. In addition to these, this paper has discussed the problem of ZCS turn-off of the auxiliary active power switch, and suggested to reduce the unnecessary parasitic oscillation with using lossless clamping diode loop. In terms of the measured voltage and current operating waveforms and EMI conducted emission, the diode clamping diode loop to suppress this high-frequency parasitic oscillation is suggested and presented herein.

References

[1] G. Hua, C.S. Leu, Y. Jiang and F.C. Lee, "Novel Zero-Voltage-Transition PWM Converters", *IEEE* Trans. Power Electronics, Vol. 9, No. 2, pp. 213-219, March. 1994.

[2] X. Yang and Z. Wang, "A Family of New Zero-Voltage-Transition PWM Converter with Zero-Current Turn off Auxiliary Switch", Proceedings of ICPE, Seoul, pp. 74-78, Oct. 1998.

[3] K.S. Park and Y.H. Kim, "New High Efficiency Zero-Voltage-Switching AC-DC Boost Converter Using Coupled Inductor and Energy Recovery Circuit", Trans. KIEE, Vol. 50B, No. 10, pp. 501-507, Oct. 2001.

[4] R. Gurunathan and A.K.S. Bhat, "Large-Signal Analysis and Simulation of a ZVT Boost Converter", Proceedings of *IEEE*-PEDS, Indonesia, pp. 425-431, Nov. 2001.

[5] K.M. Smith and K.M. Smedley, "A Comparison of Voltage-Mode Soft-Switching Methods for PWM Converter", *IEEE* Trans. Power Electronics, Vol. 12, No. 2, pp. 376-386, March. 1997.

[6] H.S. Choi and B.H. Cho, "Novel Zero-Current-Switching (ZCS) PWM Switch Cell Minimizing Additional Conduction Loss", KIEE International Trans. Electrical Machinery and Energy Conversion Systems, Vol. 12B, No. 1, pp. 37-43, March. 2002.

[7] T.F. Wu and S.A. Liang, "Systematic Approach to Developing Single-Stage Soft Switching PWM Converters", *IEEE* Trans. Power Electronics, Vol. 16, No. 5, pp. 581-593, Sept. 2001.

[8] K.M. Smith and K.M. Smedley, "Engineering Design of Lossless Passive Soft Switching Methods for PWM Converters-Part I", *IEEE* Trans. Power Electronics, Vol. 16, No. 3, pp. 336-344, May. 2001.

[9] Y. Tang, H. Zhu, B. Song, J.S. Lai and C. Chen, "EMI Experimental Comparison of PWM Inverters Between Hard- and Soft-Switching Techniques", Proceedings of VPEC Seminar, Virginia Tech. , pp. 247-253, Sept. 1998.

[10] D. Zhang, D.Y. Chen and F.C. Lee, "An Experimental Comparison of Conducted EMI Emissions between a Zero-Voltage Transition Circuit and a Hard Switching Circuit", *IEEE*-PESC Conf. Record, Italy, Vol. 2, pp. 1992-1997, June 1996.

Koki Ogura was born in Shimane, Japan. He received his B. Eng. and M. Eng. degrees in Electrical and Electronics Eng. from Yamaguchi University, Yamaguchi, Japan in 2000 and 2002, respectively. He is currently doing research in Dept. of Electrical System Engineering, the Graduate School of Science and Engineering, Yamaguchi University, Japan towards his Ph. D. degree. His research interests include the development of high frequency soft- switched resonant power conversion circuits and systems applied to new energy system such as photo voltaic generation system. He is a student member of IEEE, the Institute of Electrical Engineers of Japan, the Institute of Electronics, Information and Communication Engineers, the Japan Institute of Power Electronics and the Japan Solar Energy Society.

Srawouth Chandhaket was born in Surin, Thailand. He received his B. Eng. degree in Electronics from Kobe University, Hyogo, Japan in 1995 and also his M. S. degree in Electrical Engineering from Virginia Tech. in 1998. He is currently a Ph. D. candidate in the Graduate School of Engineering and Science, Yamaguchi University, Yamaguchi, Japan since 2001. His research interests include the soft-switching technology in power electro nics and power systems, the stability of power system network and the applications of soft computing in power electronics and power systems. He is a student member of IEEE, the Institute of Electrical Engineers of Japan and the Japan Solar Energy Society.

Tarek Ahmed received his M. S. degree from the Dept. of Elect rical Engineering, Assiut Univer sity, Egypt in 1998. He is curren tly a Ph. D. candidate student in the Graduate School of Science and Engineering, the Power Electro nic System and Control Engineering Laboratory at Yamaguchi University, Yamaguchi, Japan. His research interests are in the area of the new applications for the power electronic circuits and systems with the renewable energy and power systems and semiconductor power conditioners. Mr. Ahmed is a student member of IEEE, and the Japan Institute of Power Electronics.

Mutsuo Nakaoka was born in Hiroshima, Japan. He received his doctoral degree in Electrical Engin eering from Osaka University, Osaka, Japan in 1981. He joined in the Dept. of Electrical and Electronics Engin eering, Kobe University, Hyogo, Japan in 1981. Since 1995, he has been a professor in the Dept. of Electrical and Electronics Engineering, the Graduate School of Engineering and Science, Yamaguchi University, Yamaguchi, Japan. His research interests include circuit and control systems of power electronics, especially in soft-switching areas. Dr. Nakaoka is a member of the Institute of Electrical Engineers of Japan, the Institute of Electronics, Information and Communication Engineers of Japan, the Institute of Illumination Engineering of Japan and a senior member of IEEE.